IEEE Access
Multidisciplinary | Rapid Review | Open Access Journal

Received 20 May 2022, accepted 19 June 2022, date of publication 23 June 2022, date of current version 29 June 2022.

Digital Object Identifier 10.1109/ACCESS.2022.3185741

Novel Topology Optimization Method for Weight Reduction in Electrical Machines

BORJA LIZARRIBAR[1,2], BORJA PRIETO[1,2], MIGUEL MARTINEZ-ITURRALDE[1,2], AND GURUTZ ARTETXE[1,2]

[1]Transport and Energy Division, CEIT-Basque Research and Technology Alliance (BRTA), 20018 Donostia-San Sebastian, Spain
[2]Department of Electrical and Electronic Engineering, Universidad de Navarra, 20018 Donostia-San Sebastian, Spain

Corresponding author: Borja Lizarribar (blizarribarc@ceit.es)

This work was supported in part by the Basque Government under Agreement Hazitek ZE-2019/00030, and in part by Lancor 2000 S. Coop.

ABSTRACT This paper proposes a combined electromagnetic and mechanical topology optimization for weight reduction in electrical machines based on Finite Element Analysis (FEA) and Evolutionary Structural Optimization (ESO). The devised method is an on-off-type algorithm with adaptative mesh in which low flux density and low Von Mises stress cells are removed successively from a first machine design. With this approach, the weight of the machine can be considerably reduced without compromising the electromagnetic performance of the machine, with a reduced computation time compared to other topology optimization methods. A case study involving a 1.2 MW low-speed, permanent magnet motor is analyzed under different conditions (algorithm parameters, initial mesh, rotational speed) and used to compare the proposed method with two other topology optimization approaches.

INDEX TERMS Permanent magnet motors, optimization, topology optimization, electrical machines, ON-OFF, weight reduction, evolutionary structural optimization.

I. INTRODUCTION

Today's demanding requirements for electrical machines have led to the search for new techniques to achieve better machine performance. In this context, the study of Topology Optimization (TO) has started as an alternative approach to accomplish this objective. TO is an optimization method which is normally used in mechanical engineering for structural analysis [1]–[3], having commercial software available for this purpose [4]. However, its availability in other fields, such as electromagnetic or thermal analysis, is limited [5], [6].

Traditionally, in electrical machines, performance maximization is achieved through parametric optimization [7]. The main difference between parametric and TO is that with TO methods, it is not necessary to a priori define all the geometrical variants, which is the case with parametric optimizations. This freedom of the resulting geometry allows the machines optimized through TO methods to achieve better performances. However, although TO has countless advantages, its application to electrical machine design is limited owing to the difficulty of achieving complex geometries with conventional manufacturing techniques.

The geometrical limitations imposed by traditional fabrication can be overcome by Additive Manufacturing (AM); therefore, TO of electrical machines is gaining importance nowadays [8]–[12]. Furthermore, AM offers advantages such as material savings and assembly time reduction.

Despite not being widely applied in electromagnetics, different methods for TO of electrical machines based on FEA have been developed in the past few years. These techniques can be broadly classified into three categories: level-set, on-off and Simplified Isotropic Material with Penalization (SIMP) methods.

Level-set methods are based on the optimization of the body surface, leading to a shape focused optimization instead of a topology focused optimization. With these techniques, regions are defined as being composed of either material ($\rho = 1$) or void ($\rho = 0$), thus not allowing for intermediate states, as in other TO algorithms. To define the material-void interface at each iteration, a level-set function, $\phi(\vec{x})$, is defined and the border is set as in (1).

$$\rho = \begin{cases} 0 : \forall \vec{x} \in \Omega : \phi(\vec{x}) < 0 \\ 1 : \forall \vec{x} \in \Omega : \phi(\vec{x}) \geq 0 \end{cases} \quad (1)$$

The associate editor coordinating the review of this manuscript and approving it for publication was Diana Leitao.

Another important aspect of the level-set approach is that the optimization mesh is adaptive, that is to say, the mesh changes over each iteration. The main drawback of these methods is that they need of an additional step of "*bubble*" insertion, because on their own they are not capable of introducing void regions to change the topology of the machine [1], [13]. Examples of level-set TO applied to electrical machines can be found in [14]–[16] and an example of multimaterial approach can be found in [17].

On-off based TO techniques start by discretizing the body that is being optimized into smaller parts. This discretization can be performed with a conventional triangular or rectangular mesh [18]. As with level-set approaches, on-off methods allow only two states of the elements to be optimized. In on-off techniques, the elements (i.e., mesh cells) to be optimized are defined at the beginning of the process and they remain the same throughout the optimization - conversely, in level-set method the mesh used in the optimization changes with the iteration number. This approach can be combined with various numerical optimization algorithms, both deterministic and evolutionary, whereas level-set methods can only be used in conjunction with gradient-based algorithms. One of the most popular on-off methods is the Evolutionary Structural Optimization (ESO) [19], which consists of "*eliminating*" the mesh cells with lower influence. There is also an evolution of this method, called Bi-directional Evolutionary Structural Optimization (BESO), in which the cells can be converted from void to material. An example of a BESO optimization method is presented in [10], in which a magneto-structural optimization is presented. Some examples of on-off approaches combined with a genetic algorithm and Normalized Gaussian Nets (NGNet) [20] (an approach which can reduce the computation time in genetic algorithms for TO) can be found in [21]–[24]. The NGNets are defined as in (2) and (3), in which w is the weight vector for each Gaussian, which is defined either as $+1$ or -1, G is the value of the Gaussian at the point x and N is the number of Gaussians.

$$f(x) = \sum_{i=1}^{N} w_i b_i(x) \tag{2}$$

$$b_i(x) = \frac{G_i(x)}{\sum_{k=1}^{N} G_k(x)} \tag{3}$$

SIMP is a TO technique in which material distribution is optimized. The main difference is that the mesh cells can have intermediate densities between void and the material selected ($0 \leq \rho \leq 1$). The magnetic permeability for the SIMP method cells is often defined as in (4), in which p is the penalty factor, that normally takes values between 3 and 5.

$$\mu_r = (\mu_{Fe}(B) - \mu_{air}(B))\rho^p + \mu_{air} \tag{4}$$

The SIMP method is often combined with the Method of Moving Asymptotes (MMA) optimizer [25], which is a numerical optimization strategy for nonlinear programming. Unlike on-off approaches, SIMP techniques are not usually combined with evolutionary algorithms because of the high computational cost associated with having multiple intermediate material states. The consideration of intermediate material states - compared to binary mesh cell densities (either 0 or 1) - vastly increases the complexity of the model. Therefore, SIMP approaches are normally coupled with gradient-based procedures, with adjoint variable methods [26], [27] being the most popular, as they can significantly reduce the computation time of derivatives compared to finite difference techniques. This method has been applied to the TO of electrical machines in different scenarios, such as in the torque optimization of PMSMs [28] and in the improvement of torque characteristics of a synchronous reluctance motor [29], [30].

TABLE 1. Different to methods applied to electrical machines.

Method	Structure	Type of Analysis	Ref.
Level-set	Syn-Rel Rotor	Magnetic	[15]
Level-set	IM Rotor bars	Magnetic	[16]
Level-set	IPM Stator teeth	Magnetic	[14]
ON-OFF NGNet + GA	IPM Rotor	Magnetic	[21]
ON-OFF Multimaterial	IPM Rotor	Magnetic	[31]
ON-OFF topological der.	IPM Rotor	Magnetic	[32]
ON-OFF topological der.	SRM Stator teeth	Magnetic	[33]
SIMP + MMA	IPM Rotor	Magnetic	[28]
SIMP + GCMMA	Syn-Rel Rotor	Magnetic + Structural	[34]
SIMP + GCMMA	SRM Rotor Poles	Magnetic	[35]
SIMP	SRM Rotor + Stator teeth	Magnetic	[36]
BESO	SPM Rotor	Magnetic + Structural	[37]

A number of examples regarding previous work on TO of electrical machines are shown in Table 1, in which the presented methods are combined with different numerical optimization algorithms, such as, Genetic Algorithms (GA), MMA and its globally convergent version Globally Convergent Method of Moving Asymptotes (GCMMA). A combination with topological derivatives (topological der.) - which is the calculation of the sensitivity of each cell with respect to an objective - is also presented.

This article proposes a novel on-off ESO algorithm with adaptive meshing for weight reduction in electrical machines. The method is based on removing magnetically and mechanically "*low loaded*" mesh elements; that is, elements with low flux density and Von Mises stress values. As the mesh cells are modified according to the saturation of the material, the proposed approach is termed Saturation Method. As a control parameter, the average electromagnetic torque of the electrical machine is evaluated every iteration. If the torque

is reduced beyond a certain threshold, the optimization algorithm is stopped. The main advantage of the method proposed in this study, in comparison with other TO techniques, is the reduced computation time required to reach a weight-optimized machine. Another advantage of this method is that, although TO has been previously applied mostly to the rotor structure, the proposed approach simultaneously optimizes both the rotor and stator.

Therefore, the proposal is innovative in that both the rotor and stator are optimized simultaneously; it combines different physics in the optimization, magnetic and structural, and it uses an adaptive mesh that makes it more independent with respect to the initial mesh.

The remainder of this article is organized as follows: First, the proposed TO method is explained in detail in Section II. Once the TO method has been explained, various practical cases are analyzed in Section III. A comparative study among different TO methods is presented in Section IV. Finally, the conclusions of this study are presented in Section V.

II. DESCRIPTION OF THE SATURATION METHOD

The proposed method is an iterative algorithm that combines magneto-structural TO based on FEA and ESO, with adaptive mesh for each iteration. The suggested approach lies in reducing weight by shifting the cells magnetically and structurally less saturated from material ($\rho = 1$), to void ($\rho = 0$). The material used in this case is a ferromagnetic material, but for other optimizations, $\rho = 1$ can be defined as copper or magnet material. In this regard, the presented method is similar to the on-off + ESO approach for structural TO, with the particularity that it employs an adaptive mesh, which is a typical characteristic of level-set methods. Although the applicability of TO in electrical machines is wide, this study focuses on the TO of ferromagnetic components.

A. OPTIMIZATION PROBLEM

The optimization problem solved by this method can be defined as in (5).

$$\begin{aligned} \min \quad & G = \sum_{e=1}^{N} \rho_e V_e \\ \text{s.t.} \quad & T_{avg} \geq k_T T_{avg,0} \\ & \max(\sigma_e) \leq \sigma_{adm} \\ & \rho_e = 0 \; or \; 1 \qquad e = 1 \ldots N \end{aligned} \tag{5}$$

In the previous equation, G is the total weight of the machine; ρ_e is the density of each element, which is either 1 or 0, depending on whether the mesh element belongs to a physical material; and V_e is the volume of each element. T_{avg} is the average torque at each TO iteration, and $T_{avg,0}$ the initial average torque; that is, the average torque for a full electrical period FE simulation for the initial machine model prior to being modified by the TO algorithm. k_T is a coefficient defined by the user by which the maximum allowable reduction in torque is fixed. σ_e is the Von Mises stress of a specific element, and σ_{adm} the maximum admissible Von Mises stress for structural mechanics considerations, which is defined as the yield strength of the material used, divided by a security factor.

The problem to be solved is to minimize the total volume of the region defined as topology optimizable while ensuring that the average torque does not fall beyond an established limit and that the mechanical stress in all mesh elements is below the admissible limit.

A flowchart of the proposed TO algorithm is depicted in Fig. 1. The method starts with an initial geometry, the machine to be optimized. The initial machine geometry is divided according to an initial mesh. Once the regions are divided, the machine is evaluated electromagnetically by simulating one full electrical period and computing the average torque and the flux density in all mesh cells. Additionally, the machine is structurally computed by considering the mechanical loads due to the torque, rotational speed and magnetic forces due to the rotor-stator interaction. The cells are then sorted according to their flux density level. Starting from the magnetically least saturated cell - and progressing until the maximum allowable transformation of cells to void for each iteration is reached – each cell is subject to certain conditions. If the cell Von Mises stress is below the allowable limit (σ_{adm}), and the saturation is also below a certain established limit (B_{limit}), the cell is converted to void. Once the geometry of the next generation has been defined, it is meshed again, placing more mesh elements at the borders between void and solid material. This is done by adding one additional intermediate point to each line that defines the void-solid material border, having more elements at the void-solid material border at the next iteration. Then, the process is repeated until either the electromagnetic torque evaluated from the FEA is lower than the established limit, $k_T \cdot T_{avg,0}$, all cells have been converted into void, or the maximum number of allowed iterations has been reached.

B. PARAMETER DEFINITION

There are three main parameters that must be set in the proposed method which may affect the final geometry obtained. These parameters are the following:

- B_{limit}: Sets the maximum flux density level that one cell can have if it is to be changed to void.
- $\%_{change}$: Sets the maximum percentage of the entire optimization region that can be changed to void at each iteration.
- k_T: Limits the total reduction in torque for the final optimized machine.

III. CASE STUDY - PARAMETER TUNING

To demonstrate the working principle of the proposed method, this section presents a 2D case study on the application of the algorithm for the optimization of the ferromagnetic parts of the stator and rotor of a machine. The Saturation Method algorithm is implemented in MATLAB coupled with ALTAIR FLUX® for the electromagnetic FEA calculation.

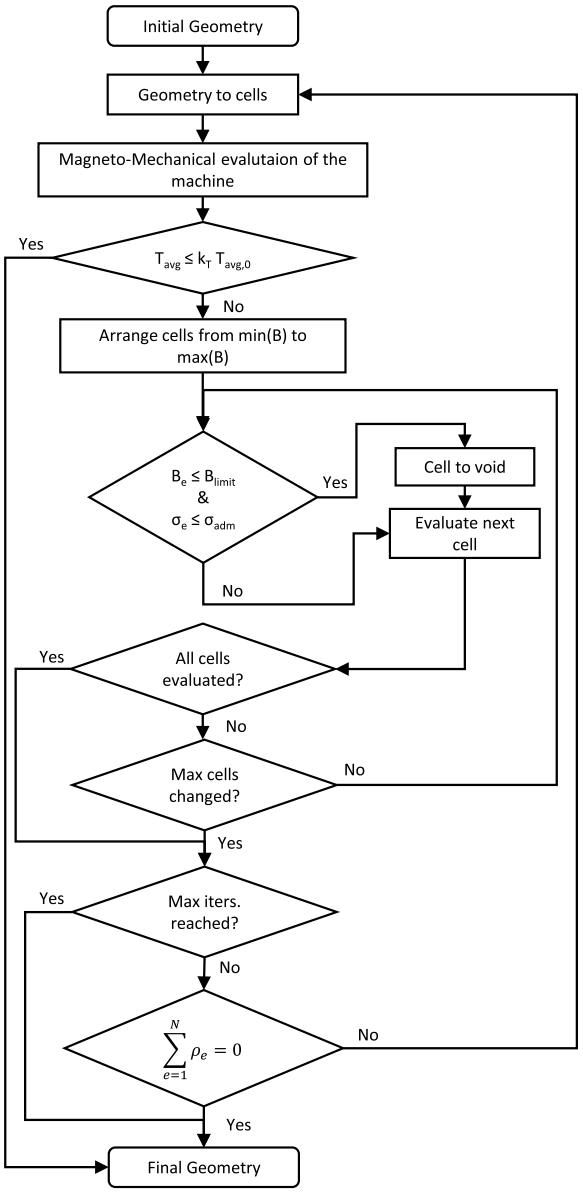

FIGURE 1. Flowchart for the proposed TO algorithm.

The mechanical calculation is performed with the PDE Toolbox of MATLAB.

A. TO PROBLEM DEFINITION

The electric machine that is used as a case study for the saturation TO algorithm is a 1.2 MW, 600-rpm, permanent magnet motor with an integral-slot distributed winding, working at 180°C and aimed at marine propulsion. A 2D sketch of the initial machine geometry is shown in Fig. 2, along with the definition of the optimizable parts. To simplify the problem and accelerate the optimization, periodic structures in the rotor and stator are defined such that the rest of the rotor and stator parts are defined based on mirror axes accordingly.

In this model, to ensure mechanical integrity, there is a frozen part in the rotor that does not change during the optimization process.

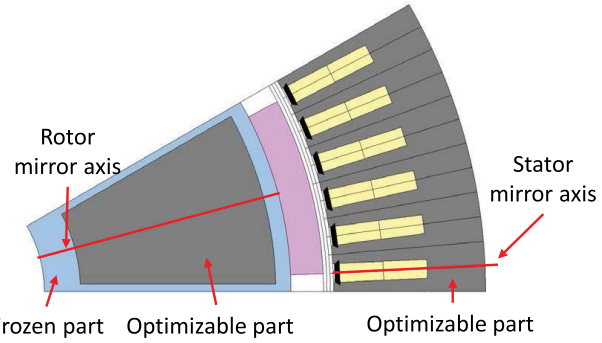

FIGURE 2. TO problem definition.

For this case study, the values of the parameters defined in Section II are as follows:

- $B_{limit,rotor} = 1.4$ T
- $B_{limit,stator} = 1.4$ T
- $\%_{change,rotor} = 5\%$
- $\%_{change,stator} = 1\%$
- $k_T = 0.99$

With the values defined, the proposed method is used for the simultaneous TO of the rotor and stator. The results of the optimization are presented in Fig. 3. For this specific case, the total torque reduction is 0.40% and the area loss of the optimizable parts is 67.5%.

It is interesting to note the mesh variation throughout the optimization process. As within the saturation method the FEM mesh is adaptative, the number of mesh elements changes in each iteration. In this case, the initial model mesh is composed of 14,631 nodes and 7,242 surface elements, whereas the final model mesh has 18,463 nodes and 9,154 surface elements. This difference in FEM mesh can be appreciated in Fig. 4, while the magnetic flux density distribution in the optimizable parts is shown in Fig. 5.

The case study proposed above finishes after 19 iterations and it takes 1 hour and 17 minutes of computation using single-core computation on an Intel® Core™ i5-6500 CPU @ 3.20 GHz. The number of steps required for the transient electromagnetic simulation is 36, and mechanically, the entire rotor is modeled owing to limitations in the MATLAB PDE Toolbox for defining periodic boundary conditions.

Finally, in Fig. 6 and Fig. 7, the torque and EMF waveforms for the initial and the optimized models respectively are shown. It can be concluded that the variation in the back-EMF waveform is almost imperceptible, while the difference in the torque profile is of less than 1% of the average torque, as expected.

B. SENSITIVITY ANALYSIS

To analyze the influence of the main parameters on the performance of the optimization algorithm, a sensitivity analysis (except for parameter k_T, which is related to the maximum allowable reduction in average torque) is carried out in this subsection.

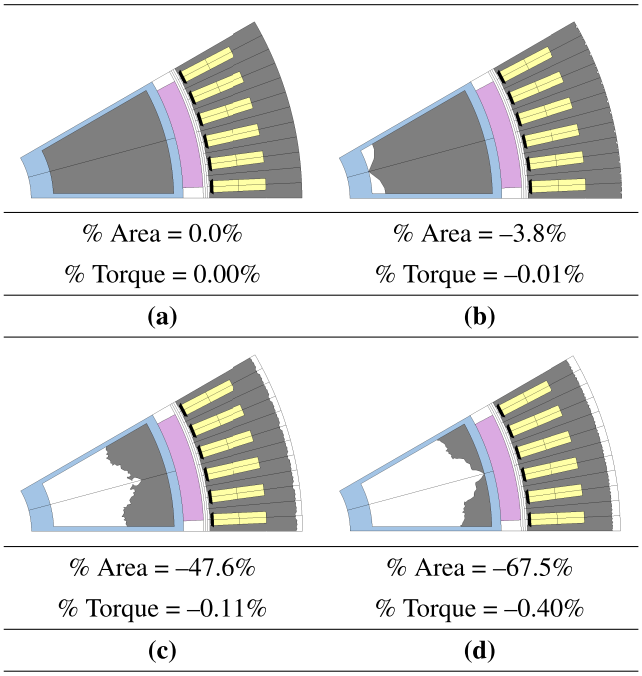

FIGURE 3. Results for case study, a) Initial model, b) 1st iteration, c) 13th iteration and d) TO result (19th iteration).

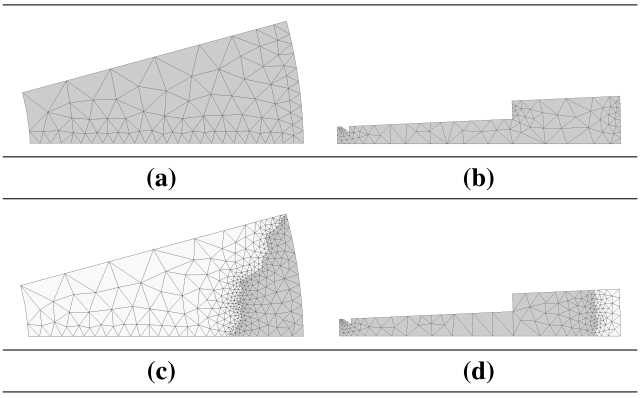

FIGURE 4. Mesh comparison, a) Initial model rotor mesh, b) Initial model stator mesh, c) Final model rotor mesh, d) Final model stator mesh.

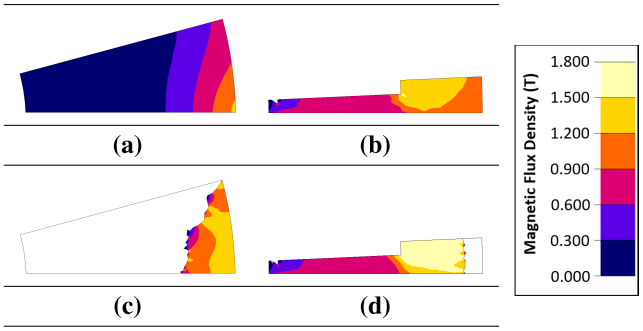

FIGURE 5. Magnetic flux density distribution at 0° rotor position, (a) Initial model rotor, (b) Initial model stator, (c) Final model rotor, (d) Final model stator.

The sensitivity analysis is performed as follows, taking as the baseline parameter-set the values defined in the previous subsection:

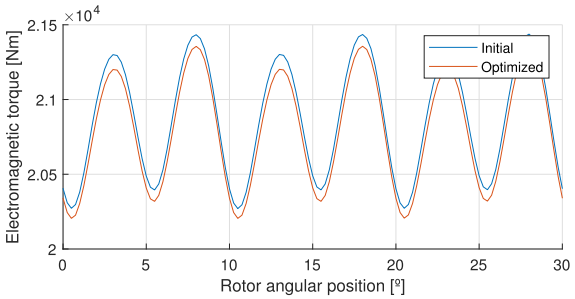

FIGURE 6. Torque profile comparison between the initial and the optimized models.

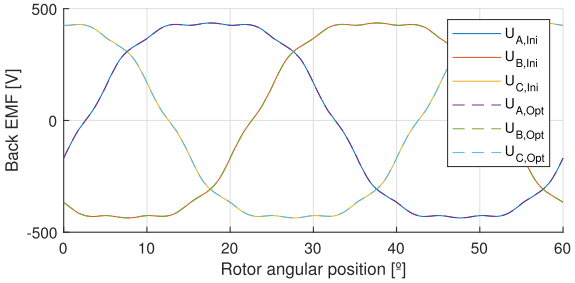

FIGURE 7. Back-EMF waveform comparison between the initial and the optimized models.

1) First, the influence of varying the flux density limits in the stator and rotor, $B_{limit,stat}$ and $B_{limit,rot}$, respectively, is analyzed. The values used for this combination are $B_{limit,stat} = [1.4, 1.6, 1.8]$ and $B_{limit,rot} = [1.4, 1.6, 1.8]$. This leads to nine combinations of parameters, the results of which are listed in Table 2. It can be observed that the change in $B_{limit,rot}$ has no influence on the results obtained for the simulation. However, when $B_{limit,stat}$ is set to its maximum value of 1.8 T, the highest reduction in area and average torque is produced. The best combination of parameters in terms of torque reduction is selected as $B_{limit,stat} = 1.4$ T and $B_{limit,rot} = 1.8$ T.
2) Once the best combination of B_{limit} is selected, a sensitivity analysis of the percentage of change allowed in each iteration is performed. As before, three cases are analyzed for both the rotor and stator, $\%_{change,stator} = [1, 2, 3]$ and $\%_{change,rotor} = [5, 10, 20]$. In Table 3 the results of these nine combinations are listed. It can be seen that the most favorable case is that with $\%_{change,stator} = 1\%$ and $\%_{change,rotor} = 10\%$.

For the specific motor analyzed, the stator is the limiting part, as $\%_{change,stator}$ has a greater influence on the torque loss than $\%_{change,rotor}$. This conclusion is valid mainly for this machine, as the stator yoke is magnetically more loaded, and a small change in it leads to a high loss in torque. It is clear that for this specific case, it is better to set a small value of $\%_{change,stator}$ so that it does not have much effect on the torque performance. Moreover, it can be extracted from Table 3 that with higher values of $\%_{change,stator}$ and $\%_{change,rotor}$ the optimization algorithm converges more rapidly, which could result in a failure to achieve the optimal solution. Taking

TABLE 2. Sensitivity analysis for different B_{limit} combinations.

$B_{limit,rot}$ \ $B_{limit,stat}$		1.4 T	1.6 T	1.8 T
1.4 T	% Area	–70.1	–72.3	–72.3
	% Torque	–0.81	–0.98	–0.96
	Number of Iterations	19	19	19
	Comp. Time [min]	77	76	78
1.6 T	% Area	–70.1	–72.3	–72.3
	% Torque	–0.81	–0.98	–0.96
	Number of Iterations	19	19	19
	Comp. Time [min]	79	76	75
1.8 T	% Area	–70.1	–72.3	–72.3
	% Torque	–0.81	–0.98	–0.96
	Number of Iterations	19	19	19
	Comp. Time [min]	76	78	77

TABLE 3. Sensitivity analysis for different $\%_{change}$ combinations.

$\%_{change,rotor}$ \ $\%_{change,stator}$		1%	2%	5%
5%	% Surface loss	–70.1	–32.6	–17.3
	% Torque loss	–0.81	–0.33	–0.78
	Number of Iterations	19	9	4
	Comp. Time [min]	78	29	15
10%	% Surface loss	–72.7	–65.7	–33.8
	% Torque loss	–0.53	–0.34	–0.78
	Number of Iterations	10	9	5
	Comp. Time [min]	39	37	19
20%	% Surface loss	–65.8	–66.4	–67.7
	% Torque loss	–0.02	–0.06	–0.79
	Number of Iterations	5	5	5
	Comp. Time [min]	18	18	19

all these considerations into account, it is clear that the optimization result is highly dependent on the parameter set used; therefore, in order to achieve the best optimization solution, an analysis of the baseline machine is needed to carefully select the parameter set by considering the magnetic saturation in the rotor and stator. The resulting shape obtained for the optimal parameter set ($B_{limit,stator}$ = 1.4 T, $B_{limit,rotor}$ = 1.8 T, $\%_{change,stator}$ = 1%, $\%_{change,rotor}$ = 10%) is presented in Fig. 8.

The results obtained for the best parameter set are promising as the weight reduction of the active parts (including the winding) after optimization is 38.4% and the torque density is improved from 11.8 Nm/kg to 19.1 Nm/kg (active). This improvement is achieved in 10 iterations, 1 hour and 12 minutes of computation time.

C. MESH DEPENDENCY

The initial mesh used has a strong influence on the final result. To analyze this dependency on the initial mesh, a comparison between two optimized machines is performed: one machine

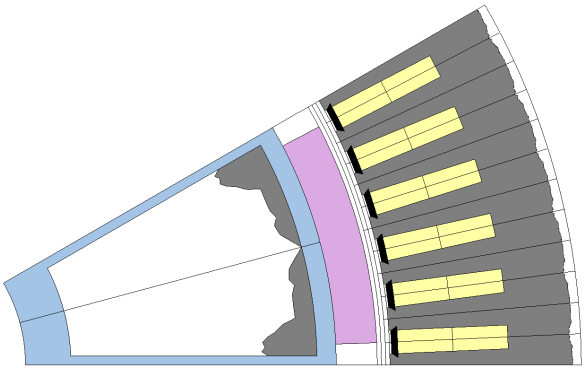

FIGURE 8. Topology optimization result for the best combination of analyzed parameters ($B_{limit,stator}$ = 1.4 T, $B_{limit,rotor}$ = 1.8 T, $\%_{change,stator}$ = 1%, $\%_{change,rotor}$ = 10%).

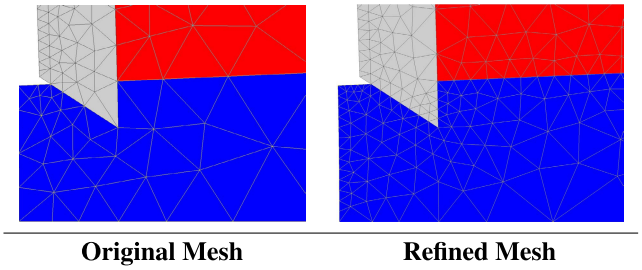

FIGURE 9. Mesh comparison between original and refined mesh.

with the mesh used in the previous sections, and the other with a refined mesh. To study this effect, the stator yoke and rotor yoke are kept frozen; therefore, the area to be analyzed is only that of the stator tooth.

The region in which the dependency on the initial mesh is most notable is where the stator tooth interferes with the stator wedge and the coils. In Fig. 9, this zone is represented. It can be seen that the size of the elements are larger in the case of the original mesh than the refined mesh model. The large size of the initial mesh elements may lead to poor resolution in the optimizable area, resulting in some of the cells not being changed from iron to void. Fig. 10 shows that the vast majority of the stator is above the imposed limit of 1.4 T. Further, in this figure there is a zone adjacent to the coil, in which the magnetic flux density is lower than 1.4 T, which is the B_{limit} established. However, due to the large size of the mesh elements, the two elements that cover this region have an average magnetic flux density in the element higher than the B_{limit}. In this scenario, it can be assumed that if smaller elements are predefined (such as in Fig. 9) additional cells could be changed from iron to void.

The resultant shapes obtained after the optimization of the two different initial meshes are shown in Fig. 11. It can be observed that the final results obtained with the two meshes are clearly different. As expected, in the refined mesh model (that uses smaller size elements) the TO program is able to change the elements that are in contact with the coils and stator wedge from iron to void unlike in the case of the original meshing.

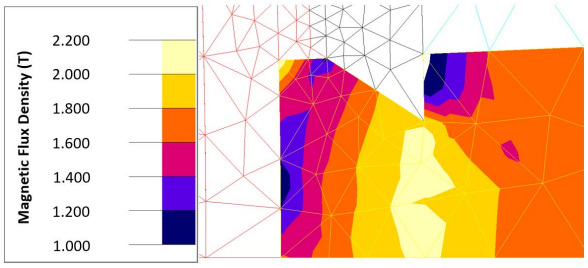

FIGURE 10. Magnetic flux density distribution with the original mesh.

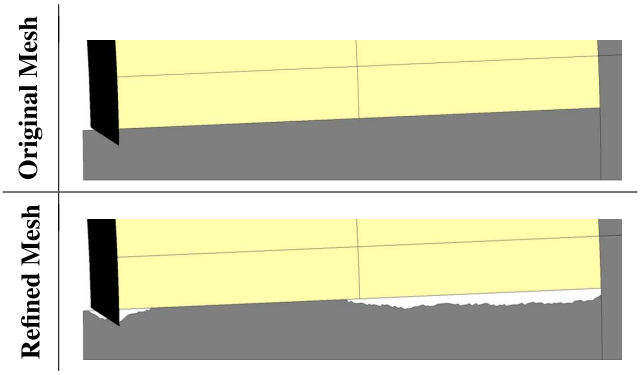

FIGURE 11. Optimization results for the original and the refined mesh models.

With mesh refinement, 9.2% of the stator tooth is changed from iron to void. However, an increase in computation time is required - 2 hours 20 minutes in the refined model compared with 1 hour 20 minutes for the original model. This increase in computation time is due to the higher number of mesh elements in the refined model, 925 mesh nodes in half a stator tooth, compared to 131 nodes in the original one. Thus, it is clear that a trade-off between the optimization accuracy and the computation time must be achieved.

D. EFFECT OF THE MECHANICAL LOADS

As previously mentioned, the analyzed machine operates at a low speed and, therefore, the mechanical stresses in the machine are far from the yield strength. In order to study the behavior of the algorithm with higher loads, a higher speed of 6,000 rpm is considered in this subsection. The radial centrifugal force acting at the rotor is defined as in (6), where N is the number of elements, m_e and ρ_e are the mass and the density of the element, respectively, ω is the angular speed and R_e is the radius of the center of gravity of the element.

$$F_{rad} = \sum_{e=1}^{N} m_e \rho_e \omega^2 R_e \tag{6}$$

It has been previously exposed that for the analyzed case study the stator cells are the most sensitive to the torque limit, owing to the higher saturation of the stator structure. To ensure that just the rotor behavior is analyzed, the parameter $B_{limit,stat}$ is set to 0, so no cells of the stator are changed to void and the algorithm is not influenced by them. Moreover, to have smooth shapes in the rotor and to ensure mechanical

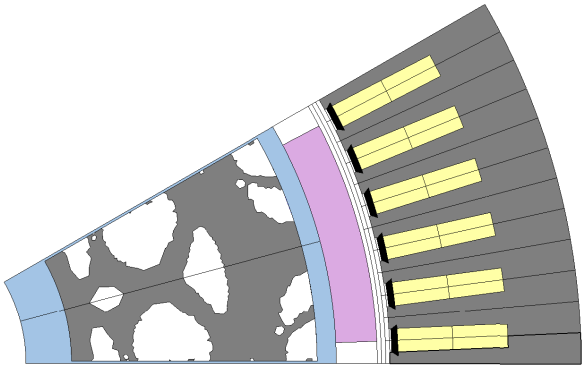

FIGURE 12. Optimization resultant shape with 6,000 rpm.

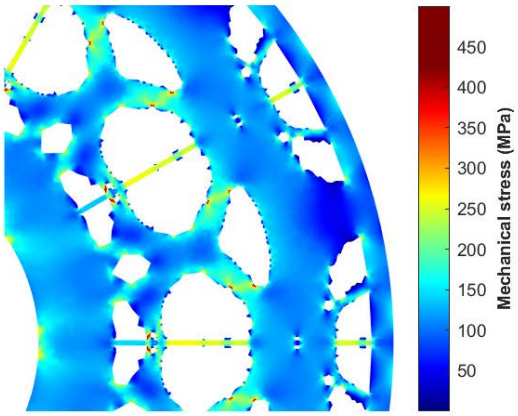

FIGURE 13. Mechanical stress distribution in one rotor pole.

strength, the parameter $\%_{change}$ of the rotor is set to 1%. Finally, the frozen part of the rotor has been set thinner than in previous sections so that the predefined walls are not able to support the rotor structure by themselves.

The FEM model of the optimized machine is shown in Fig. 12. It is clear that due to the high centrifugal forces that are now applied, the resultant shape of the rotor varies from the ones obtained for the previous analyses. This is due to the higher stresses inside the rotor, which limit the transition of some cells from iron to void.

In this specific case, it is also interesting to analyze the mechanical behavior of the optimized machine. The results of the mechanical analysis are represented in Fig. 13. The yield strength of the considered electrical steel (i.e. M600-65A) is 300 MPa. In the previous figures, it can be noticed that at some points, the stress limit is reached. This stress concentration appears at the edges and is due to the effect of having sharp corners at the edges.

To eliminate the distortion caused by the stress concentration, a smoothing of the edges of the resultant shape is applied. This smoothing is performed by approximating the curves that define the border of the rotor material via a 3rd order polynomial curve. The final smoothed geometry is shown in Fig. 14; along with its corresponding mechanical analysis in Fig. 15. Compared with the shape depicted in

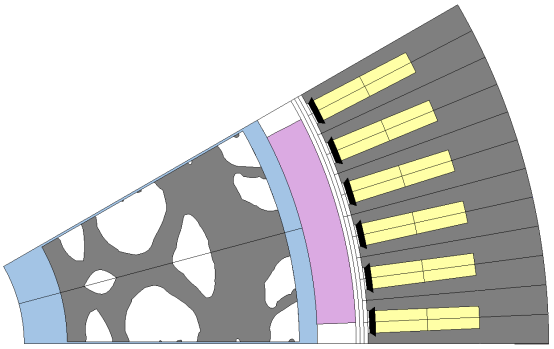

FIGURE 14. Smoothed shape of the resultant optimization.

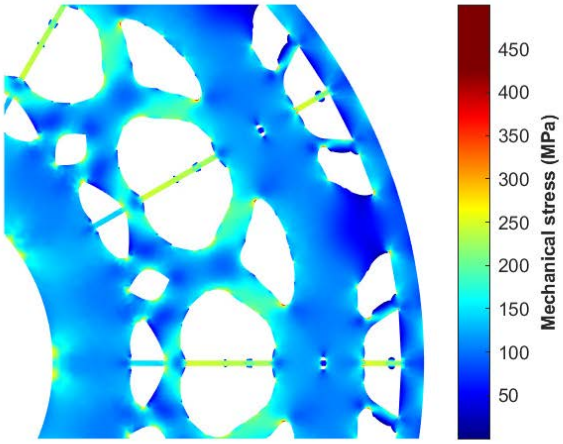

FIGURE 15. Mechanical stress distribution for the smoothed TO rotor.

Fig. 13, it is clear that most of the stress concentration zones are removed by this technique.

The proposed optimization is performed in 16 iterations for 1 hour and 52 minutes. The reduction in torque is 0.68% and the decrease in the optimizable area is 39.3%. The initial model mesh is composed of 17,416 nodes and 8,545 surface elements and the mesh of the final model has 23,292 nodes and 11,495 surface elements. The total weight of the active parts is reduced by 20.2%, and mechanical stability is ensured.

It is clear from the results of the subsection that when the loads inside the rotor increase, the algorithm starts behaving more like a mechanical TO than a electromagnetic TO. Another fact that is worth commenting on is that the parameter $\%_{change,rotor}$ appears to be very significant; as if this parameter is above a threshold, the quantity of material removed by each iteration can be large and the mechanical stresses inside the rotor can have higher values than the permitted ones. Thus, for highly loaded rotors, it is necessary to define a lower $\%_{change,rotor}$.

Finally, the torque and EMF waveforms for the initial and the optimized model are shown in Fig. 16 and Fig. 17. Same as in subsection III-A, it is seen that the difference in the Back-EMF waveform is nonexistent and in the torque is of less than 1%.

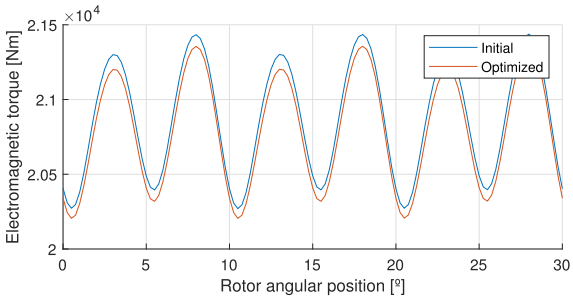

FIGURE 16. Torque profile comparison between the initial and the optimized models.

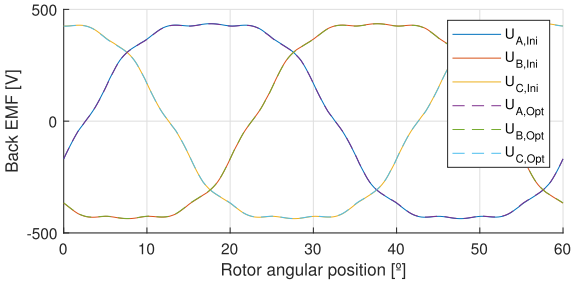

FIGURE 17. Back-EMF waveform comparison between the initial and optimized models.

Finally, the torque and EMF waveforms for the initial and the optimized models are shown in Fig. 16 and Fig. 17, respectively. In the same fashion as in subsection III-A, it is seen that the difference in the Back-EMF waveform is almost nonexistent, whereas the reduction in the average torque is less than the 1%.

IV. COMPARATIVE STUDY

To compare the proposed method with other TO approaches, in this subsection two different TO algorithms are applied to the same machine. The two methods selected are based on SIMP and on-off approaches.

A. SIMP

The SIMP algorithm used for the TO of the motor has been based on [26] and combined with the MMA optimizer proposed in [25]. In most of the previous work, the optimization objective has been torque related. Despite this, in the present work the optimization objective is to minimize the total rotor area subject to a reduction in torque of less than 1%. This modification of the objective function has been applied to perform a fair comparison between the proposed and SIMP methods.

For the optimization via the SIMP approach, the rotor symmetry has not been defined, the simulation has been defined as magnetostatic, and the number of electromagnetic simulation steps has been reduced from 36 to 6, and the mechanical calculation is not performed. These modifications in the simulation setup are carried out to achieve results more rapidly, as the method requires the computation of the derivatives of each element with respect to the objective function, which is a very costly process in terms of computation time,

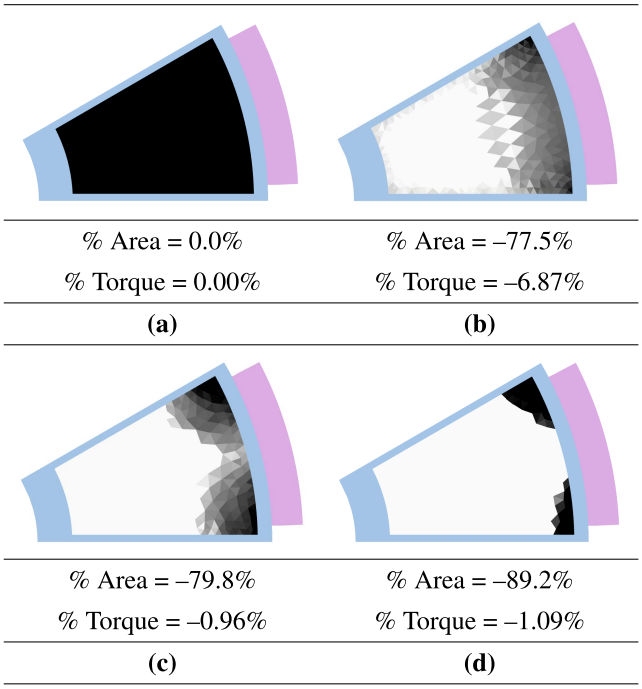

FIGURE 18. Results for the SIMP TO, a) Initial model, b) 5th iteration, c) 10th iteration and d) TO result (158th iteration).

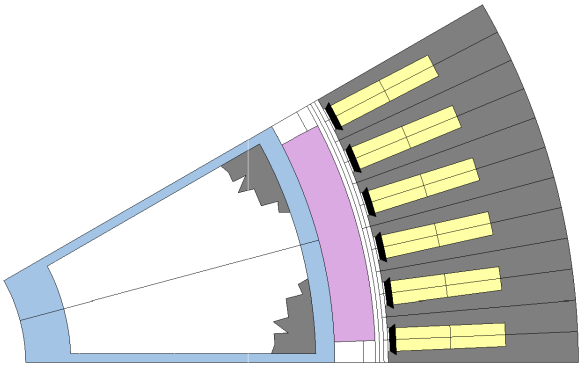

FIGURE 19. Resultant shape obtained by the on-off optimization.

TABLE 4. TO method comparison.

Method	Comp. time	Iterations	Structural Analysis	Area loss Rotor TO
Saturation	1h 12min[a]	10	Yes	82.7%
SIMP	21h 30min[b]	158	No	89.2%
On-off	96h 00min[b]	11,814	No	89.3%

[a]Time required for a transient electromagnetic simulation of 36 steps + mechanical analysis for each design candidate.

[b]Time required for a magnetostatic electromagnetic simulation of 6 steps for each design candidate

consuming approximately 93% of the time needed for each iteration in the case studied.

The results of applying the SIMP algorithm to the case study are shown in Fig. 18. In this figure, the main characteristic of the SIMP method, that is that the material may have intermediate density states (black color: 100% density, white color: 0% density), can be seen. For the in-between iterations, (b) and (c), some intermediate material zones are observed. However, in the converged solution, the intermediate material states have almost disappeared.

TO by the SIMP algorithm has required 158 iterations, 21 hours and 30 minutes to reach the converged solution.

B. ON-OFF

The second additional TO approach that is analyzed is an on-off method combined with a Multi-Objective Differential Evolution (MODE) [38] coupled with an NGNet + greedy algorithm from [20] to reduce the required computation time.

Following the same reasoning as for the SIMP method, the calculation steps are reduced to 6 and the electromagnetic simulation is set as magnetostatic, without a mechanical computation.

Contrary to the other two presented methods, in which there is a single optimization objective (area reduction), the optimization results for this method are given in terms of a Pareto front for the area and torque reduction, as the programmed algorithm is multi-objective. Therefore, to have a fair comparison among methods, the machine of the Pareto front with an average torque closer to the 99% of the initial torque is selected.

The resultant shape obtained using this method is illustrated in Fig. 19. It leads to a torque reduction of 1% and an area loss of the optimizable area of 89.3%. The on-off optimization has converged in 96 hours and it has required 11,814 simulations. It should be noted that the computation time could be reduced by relaxing the convergence criteria or reducing the number of Gaussians defined to perform the optimization, 55 in the analyzed case.

C. COMPARISON

A summary of the main results obtained by the different TO methods is presented in Table 4.

Table 4 shows the main advantages and disadvantages of the proposed algorithm compared with other algorithms found in the literature. The main disadvantage of the saturation approach is that the flexibility of the presented method for optimizing objective functions other than the weight is limited. However, with other methods, such as on-off + genetic algorithms, the number of objectives and their nature can vary significantly.

On the other hand, the most noticeable advantage is the computation time of each optimization algorithm. The saturation method requires a much shorter computation time compared to the other two methods, despite the higher number of calculation steps used for the presented approach and using transient calculation, which normally requires a longer computation time. This is due to the faster convergence of the proposed algorithm, which converges to a local optimum instead of a global optimum point. This can also be seen in the lower area reduction of the rotor TO zone in the saturation

method compared with the other two methods. Nevertheless, the area reduction is of the same order of magnitude, with a much shorter computation time.

Another advantage of the proposed algorithm is the multiphysics (magneto-structural) nature of the optimization, which can achieve magnetically and mechanically optimized structures, as shown in Fig. 14. Multiphysics optimization can be performed using SIMP approaches, as in [27] and [39], although a previous electromagnetic optimization is performed, and once a magnetically functional structure is achieved, a magneto-structural optimization is applied. For on-off methods with multi-objective algorithms, literature on magneto-structural optimization has not been found.

Regarding the adaptive mesh defined in the proposed algorithm, there is an advantage of a much smoother material to void frontier compared to the resultant shapes of the optimization via SIMP and on-off methods. In addition, as the mesh in the saturation approach changes in each iteration, it is more initial mesh independent than the other two methods in which the same mesh is used for the whole TO process.

Finally, one last advantage of the saturation approach is the possibility of simultaneously optimizing the rotor and stator structures. An example of a simultaneous TO is found in [36], in which the rotor and the stator teeth are magnetically optimized, but not the stator yoke. In the related literature, TO methods are mainly focused on rotor optimization and, in some cases, just on the stator optimization.

V. CONCLUSION

This study presents a novel TO method based on FEA and ESO with an adaptive mesh. The algorithm is proven effective for reducing the weight of an electrical machine without losing performance characteristics. The algorithm has been tested with a case study in which an improvement in torque density of active parts from 11.8 Nm/kg to 19.1 Nm/kg has been achieved. The influence of the initial mesh on the stator tooth geometry has also been studied, highlighting its importance in the final result. The TO approach has proven to be valid for the optimization of high speed rotors, leading to a weight reduction of 20.2% of the motors active parts. Finally, a comparison between different TO methods has been conducted, presenting the main advantages and disadvantages of the proposed TO approach.

The main advantage of this optimization method compared to alternative methods used in TO is the reduced computation time. The analyzed algorithm can achieve its final results within 20-30 FEM simulations, whereas other methods require thousands of simulations, depending on the particular case. Another particularity of the proposed approach is the simultaneous optimization of the rotor and stator.

A drawback of the devised method is that optimized solutions may converge to local optimums instead to global optimum points, as the search space is constrained to just removing material, without having the possibility of adding it. Another limitation of the presented technique is that it is just oriented to reducing the weight of the materials and not to improving other machine performance characteristics (e.g. efficiency, torque ripple, etc.).

As with other TO approaches, the final geometries derived from the optimization may be difficult to accomplish via traditional manufacturing methods. In this regard, additive manufacturing (AM) of electrical machine parts is a game-changer, which opens up the possibility of having highly optimized machine structures with additional potential gains in terms of material savings and assembly time reduction.

Future work regarding the proposed TO method involves testing the algorithm with 3D structures, demonstrating its capability to optimize copper and magnets, combining the optimizaton of different physics (such as electromagnetic-thermal), and the adoption of distinct functions for arranging the cells to be converted to void, instead of the flux density used at this moment, such as the current density for copper optimization cases.

REFERENCES

[1] H. A. Eschenauer, V. V. Kobelev, and A. Schumacher, "Bubble method for topology and shape optimization of structures," *Struct. Optim.*, vol. 8, no. 1, pp. 42–51, Aug. 1994, doi: 10.1007/BF01742933.
[2] M. P. Bendsøe and N. Kikuchi, "Generating optimal topologies in structural design using a homogenization method," *Comput. Method Appl. Mech. Eng.*, vol. 71, no. 2, pp. 197–224, 1988.
[3] D. Jankovics, H. Gohari, M. Tayefeh, and A. Barari, "Developing topology optimization with additive manufacturing constraints in ANSYS," *IFAC-PapersOnLine*, vol. 51, no. 11, pp. 1359–1364, Jan. 2018. [Online]. Available: https://www.sciencedirect.com
[4] *ANSYS Topology Optimization*. Accessed: Feb. 21, 2020. [Online]. Available: https://www.ansys.com/applications/topology-optimization
[5] *JMAG Topology Optimization* Accessed: Feb. 21, 2020. [Online]. Available: https://www.jmag-international.com/catalog/257_ipm-topologyoptimization/
[6] S. Xue and V. Acharya, "Topology optimization empowers the design of interior permanent magnet (IPM) motors," in *Proc. IEEE Transp. Electrific. Conf. Expo (ITEC)*, Jun. 2020, pp. 1–5.
[7] A. N. Gorozhankin, M. A. Grigor'ev, A. M. Zhuravlev, and D. A. Sychev, "Parametric optimization of a synchronous electric drive with improved mass and size parameters," *Russian Electr. Eng.*, vol. 86, no. 12, pp. 697–699, Dec. 2015, doi: 10.3103/S1068371215120081.
[8] N. Simpson and P. H. Mellor, "Additive manufacturing of shaped profile windings for minimal AC loss in electrical machines," in *Proc. IEEE Energy Convers. Congr. Expo. (ECCE)*, Sep. 2018, pp. 5765–5772.
[9] C. Wohlers, P. Juris, S. Kabelac, and B. Ponick, "Design and direct liquid cooling of tooth-coil windings," *Elect. Eng.*, vol. 100, pp. 2299–2308, Jul. 2018.
[10] M. Garibaldi, "Laser additive manufacturing of soft magnetic cores for rotating electrical machinery: Materials development and part design," Ph.D. dissertation, Dept. Aerosp. Technol. Centre, Univ. Nottingham, Nottingham, U.K., Dec. 2018.
[11] Z.-Y. Zhang, K. J. Jhong, C.-W. Cheng, P.-W. Huang, M.-C. Tsai, and W.-H. Lee, "Metal 3D printing of synchronous reluctance motor," in *Proc. IEEE Int. Conf. Ind. Technol. (ICIT)*, Mar. 2016, pp. 1125–1128.
[12] M. Mapley, J. P. Pauls, G. Tansley, A. Busch, and S. D. Gregory, "Selective laser sintering of bonded magnets from flake and spherical powders," *Scripta Mater.*, vol. 172, pp. 154–158, Nov. 2019.
[13] M. Y. Wang, X. Wang, and D. Guo, "A level set method for structural topology optimization," *Comput. Methods Appl. Mech. Eng.*, vol. 192, nos. 1–2, pp. 227–246, Jan. 2003. [Online]. Available: https://www.sciencedirect.com/science/article/pii/S0045782502005595
[14] J. S. Choi, K. Izui, S. Nishiwaki, A. Kawamoto, and T. Nomura, "Topology optimization of the stator for minimizing cogging torque of IPM motors," *IEEE Trans. Magn.*, vol. 47, no. 10, pp. 3024–3027, Oct. 2011.
[15] Y. Sun Kim and I. Han Park, "Topology optimization of rotor in synchronous reluctance motor using level set method and shape design sensitivity," *IEEE Trans. Appl. Supercond.*, vol. 20, no. 3, pp. 1093–1096, Jun. 2010.

[16] G. Lee, S. Min, and J.-P. Hong, "Optimal shape design of rotor slot in squirrel-cage induction motor considering torque characteristics," *IEEE Trans. Magn.*, vol. 49, no. 5, pp. 2197–2200, May 2013.
[17] P. Putek, P. Paplicki, and R. Pałka, "Topology optimization of rotor poles in a permanent-magnet machine using level set method and continuum design sensitivity analysis," *COMPEL: Int. J. Comput. Math. Electr. Electron. Eng.*, vol. 33, no. 3, pp. 711–728, Apr. 2014.
[18] Z. Fei and Y. Rongge, "Topology optimization of magnetic actuator using the improved ON/OFF method," in *Proc. 6th Int. Conf. Electromagn. Field Problems Appl.*, Jun. 2012, pp. 1–4.
[19] O. M. Querin, G. P. Steven, and Y. M. Xie, "Evolutionary structural optimisation (ESO) using a bidirectional algorithm," *Eng. Comput.*, vol. 15, no. 8, pp. 1031–1048, 1998.
[20] T. Sato, K. Watanabe, and H. Igarashi, "Multimaterial topology optimization of electric machines based on normalized Gaussian network," *IEEE Trans. Magn.*, vol. 51, no. 3, pp. 1–4, Mar. 2015.
[21] Y. Hu, Y. Xiao, B. Chen, and Q. Li, "Topology optimization of a consequent-pole rotor with V-shaped magnet placement," in *Proc. 21st Int. Conf. Electr. Mach. Syst. (ICEMS)*, Oct. 2018, pp. 234–239.
[22] S. Xue and V. Acharya, "Topology optimization empowers the design of interior permanent magnet (IPM) motors," in *Proc. IEEE Transp. Electrific. Conf. Expo (ITEC)*, Jun. 2020, pp. 1–5.
[23] I. Lolova, J. Barta, G. Bramerdorfer, and S. Silber, "Topology optimization of line-start synchronous reluctance machine," in *Proc. 19th Int. Conf. Mechatronics-Mechatronika (ME)*, Dec. 2020, pp. 1–7.
[24] J. Barta, L. Knebl, G. Bramerdorfer, I. Lolova, S. Silber, and O. Vitek, "Topology optimization of rotor bars geometry and arrangement for a line-start permanent magnet synchronous machine," *IEEE Access*, vol. 9, pp. 115192–115204, 2021.
[25] K. Svanberg, "The method of moving asymptotes—A new method for structural optimization," *Int. J. Numer. Methods Eng.*, vol. 24, no. 2, pp. 359–373, 1987. [Online]. Available: https://onlinelibrary.wiley.com/doi/abs/10.1002/nme.1620240207
[26] E. Sayed, M. Bakr, B. Bilgin, and A. Emadi, "Adjoint-based design optimization of nonlinear switched reluctance motors," *Electr. Power Compon. Syst.*, vol. 47, pp. 1705–1716, Mar. 2020.
[27] F. Guo and I. P. Brown, "Simultaneous magnetic and structural topology optimization of synchronous reluctance machine rotors," *IEEE Trans. Magn.*, vol. 56, no. 10, pp. 1–12, Oct. 2020.
[28] A. N. A. Hermann, N. Mijatovic, and M. L. Henriksen, "Topology optimisation of PMSM rotor for pump application," in *Proc. XXII Int. Conf. Electr. Mach. (ICEM)*, Sep. 2016, pp. 2119–2125.
[29] A. Credo, G. Fabri, M. Villani, and M. Popescu, "Adopting the topology optimization in the design of high-speed synchronous reluctance motors for electric vehicles," *IEEE Trans. Ind. Appl.*, vol. 56, no. 5, pp. 5429–5438, Sep. 2020.
[30] Y. Okamoto, R. Hoshino, S. Wakao, and T. Tsuburaya, "Improvement of torque characteristics for a synchronous reluctance motor using MMA-based topology optimization method," *IEEE Trans. Magn.*, vol. 54, no. 3, pp. 1–4, Mar. 2018.
[31] T. Ishikawa, S. Mizuno, and N. Krita, "Topology optimization method for asymmetrical rotor using cluster and cleaning procedure," *IEEE Trans. Magn.*, vol. 53, no. 6, pp. 1–4, Jun. 2017.
[32] P. Gangl and U. Langer, "Topology optimization of electric machines based on topological sensitivity analysis," *Comput. Vis. Sci.*, vol. 15, no. 6, pp. 345–354, Dec. 2012.
[33] E. Sayed, M. H. Bakr, B. Bilgin, and A. Emadi, "Gradient-based design optimization of a switched reluctance motor for an HVAC application," in *Proc. IEEE Transp. Electrific. Conf. Expo (ITEC)*, Jun. 2020, pp. 1031–1037.
[34] A. Manninen, J. Keränen, J. Pippuri-Mäkeläinen, S. Metsä-Kortelainen, T. Riipinen, and T. Lindroos, "Topology optimization for additive manufacturing of switced reluctance machines," in *Proc. 18th Biennial IEEE Conf. Electromagn. Field Comput. (CEFC)*, Hangzhou, China, Oct. 2018.
[35] A. Manninen, J. Keranen, J. Pippuri-Makelainen, T. Riipinen, S. Metsa-Kortelainen, and T. Lindroos, "Impact of topology optimization problem setup on switched reluctance machine design," in *Proc. 22nd Int. Conf. Comput. Electromagn. Fields (COMPUMAG)*, Jul. 2019, pp. 1–4.
[36] J. Lee, J. H. Seo, and N. Kikuchi, "Topology optimization of switched reluctance motors for the desired torque profile," *Struct. Multidisciplinary Optim.*, vol. 42, no. 5, pp. 783–796, 2010.
[37] M. Garibaldi, C. Gerada, I. Ashcroft, and R. Hague, "Free-form design of electrical machine rotor cores for production using additive manufacturing," *J. Mech. Des.*, vol. 141, no. 7, Jul. 2019, Art. no. 071401.
[38] R. Storn and K. Price, "Differential evolution—A simple and efficient heuristic for global optimization over continuous spaces," *J. Global Optim.*, vol. 11, pp. 341–359, 1997, doi: 10.1023/A:1008202821328.
[39] C. Lee, J. Lee, and I. G. Jang, "Topology optimization for the manufacturable and structurally safe synchronous reluctance motors with multiple iron webs and bridges," *IEEE Trans. Ind. Electron.*, early access, Feb. 9, 2022, doi: 10.1109/TIE.2022.3148751.

BORJA LIZARRIBAR was born in San Sebastian, Spain, in 1996. He received the B.S. and M.Sc. degrees in industrial engineering from the University of Navarra, San Sebastian, in 2018 and 2020, respectively, where he is currently pursuing the Ph.D. degree, with a focus on topology optimization of electrical machines and additive manufacturing of electrical machines.

He has participated in three research projects and is an author of one communication in an international conference.

BORJA PRIETO was born in San Sebastian, Spain, in 1987. He received the M.Sc. degree in industrial engineering and the Ph.D. degree in applied engineering from the University of Navarra, San Sebastian, in 2010 and 2015, respectively.

Since 2015, he has been a Lecturer of renewable energies and electrical systems with the University of Navarra. Since 2011, he has been conducting research activities within CEIT—a nonprofit research center, San Sebastian. He has participated in more than 25 research projects and is coauthor of eight indexed journal articles, four communications in international conferences, and three intellectual property registrations. His research interests include design and control of electrical machines, fault-tolerant PM motors, and high-power density drives.

MIGUEL MARTINEZ-ITURRALDE received the degree in industrial engineering and the Ph.D. degree from the University of Navarra, in 2001 and 2005, respectively.

He has been a Lecturer of electrical engineering with the University of Navarra, since 2006. He is an Associate Director of the Transport and Energy Division with CEIT-BRTA. He has been involved in more than 40 research projects supported by public and private funding. He is author or coauthor of 22 articles in journals and 25 communications in international conferences. His main research interests include design and control of electrical machines for transport applications.

GURUTZ ARTETXE was born in San Sebastian, Spain, 1988. He received the M.Sc. degree in industrial electronic and automatic engineering from the University of the Basque Country (UPV/EHU), Bilbao, Spain, and the Ph.D. degree in applied engineering from the University of Navarra, San Sebastian, Spain, in 2012 and 2018, respectively.

Since 2012, he has been a Researcher with the Transport and Energy Division, CEIT-BRTA, San Sebastian. He has participated in more than 20 research projects and is coauthor of five indexed journal articles and one communication in an international conference. His main research interests include the multiphysics design and control of electrical machines.